BIOLOGY OF REPRODUCTION (2012) **86**(1):14, 1–14
Published online before print 5 October 2011.
DOI 10.1095/biolreprod.111.094037

Participation of the Cl^-/HCO_3^- Exchangers SLC26A3 and SLC26A6, the Cl^- Channel CFTR, and the Regulatory Factor SLC9A3R1 in Mouse Sperm Capacitation[1]

Julio C. Chávez,[3] Enrique O. Hernández-González,[4] Eva Wertheimer,[5] Pablo E. Visconti,[5] Alberto Darszon,[3] and Claudia L. Treviño[2,3]

[3]*Departamento de Genética del Desarrollo y Fisiología Molecular, Instituto de Biotecnología-Universidad Nacional Autónoma de México, Cuernavaca, México*
[4]*Departamento de Biología Celular, Centro de Investigación y de Estudios Avanzados del Instituto Politécnico Nacional, México D.F., México*
[5]*Department of Veterinary and Animal Science, University of Massachusetts, Amherst, Massachusetts*

ABSTRACT

Sperm capacitation is required for fertilization and involves several ion permeability changes. Although Cl^- and HCO_3^- are essential for capacitation, the molecular entities responsible for their transport are not fully known. During mouse sperm capacitation, the intracellular concentration of Cl^- ($[Cl^-]_i$) increases and membrane potential (Em) hyperpolarizes. As in noncapacitated sperm, the Cl^- equilibrium potential appears to be close to the cell resting Em, opening of Cl^- channels could not support the $[Cl^-]_i$ increase observed during capacitation. Alternatively, the $[Cl^-]_i$ increase might be mediated by anion exchangers. Among them, SLC26A3 and SLC26A6 are good candidates, since, in several cell types, they increase $[Cl^-]_i$ and interact with cystic fibrosis transmembrane conductance regulator (CFTR), a Cl^- channel present in mouse and human sperm. This interaction is known to be mediated and probably regulated by the Na^+/H^+ regulatory factor-1 (official symbol, SLC9A3R1). Our RT-PCR, immunocytochemistry, Western blot, and immunoprecipitation data indicate that SLC26A3, SLC26A6, and SLC9A3R1 are expressed in mouse sperm, localize to the midpiece, and interact between each other and with CFTR. Moreover, we present evidence indicating that CFTR and SLC26A3 are involved in the $[Cl^-]_i$ increase induced by db-cAMP in noncapacitated sperm. Furthermore, we found that inhibitors of SLC26A3 (Tenidap and 5099) interfere with the Em changes that accompany capacitation. Together, these findings indicate that a CFTR/SLC26A3 functional interaction is important for mouse sperm capacitation.

capacitation, chloride channels, chloride transporters, fertilization, membrane potential, sperm, sperm capacitation, sperm motility and transport

INTRODUCTION

Fertilization requires the fusion of male and female gametes to create a new individual. Spermatozoa can fertilize the egg only after undergoing capacitation [1]. Sperm capacitation is a complex process that involves the onset of motility, changes in intracellular ion concentrations, intracellular pH (pH_i) elevation, plasma membrane hyperpolarization, and protein tyrosine phosphorylation, among other changes [2]. The increase in tyrosine phosphorylation observed during capacitation is downstream of the activation of the bicarbonate (HCO_3^-)-dependent soluble adenylate cyclase (SACY) [3] and protein kinase A (PKA) [4]. How HCO_3^- increases inside spermatozoa is not well understood. Our group [5] presented evidence strongly suggesting that HCO_3^- transport in these cells is mediated, at least in part, by a member of the Na^+/HCO_3^- cotransporter (NBC) family [6]. Upon HCO_3^- addition to the external media, this electrogenic transporter hyperpolarizes mouse sperm and causes a pH_i increase and cAMP elevation [5]. However, this NBC is not sufficient to sustain the HCO_3^-- and cAMP-dependent pathways necessary for the slow increase in other capacitation parameters, such as tyrosine phosphorylation.

Recently, we and others [7–10] have also demonstrated that Cl^- is necessary for capacitation-associated processes, such as the increase in tyrosine phosphorylation, the preparation for a physiologically induced acrosome reaction (AR), motility hyperactivation, hyperpolarization, and in vitro fertilization. Considering that Cl^- is needed for subsequent cAMP-dependent processes, we postulated that inward translocation of Cl^- is coupled to the activity of an electroneutral Cl^-/HCO_3^- cotransporter; inward fluxes of HCO_3^- through this exchanger would stimulate SACY and increase cAMP levels [3, 11].

$[Cl^-]_i$ levels are determined by the relative contributions of all Cl^- transporters present in the plasma membrane of a given cell type. Cl^- can be transported through various systems across the plasma membrane including different types of Cl^- channels and a series of specialized carriers. Cl^- channels are a subset of ion channels selective to Cl^- and often permeable to other small monovalent anions [12]. Among these channels, we and others have shown that spermatozoa have cystic fibrosis transmembrane conductance regulator (CFTR), and that this Cl^- channel is involved in the regulation of sperm hyperpolarization [9, 10]. However, considering that in spermatozoa the Cl^- equilibrium potential (Em_{Cl^-}) (−32 mV) is close to the cell membrane potential (Em) (−40 mV), the opening of any Cl^- channel (including CFTR) would not result in a considerable Cl^- influx into spermatozoa. Therefore, CFTR

[1]Supported by National Institutes of Health grants R01 HD44044 and HD038082-07A1 to P.E.V., Consejo Nacional de Ciencia y Tecnología (CONACyT-Mexico) grant 79921 to E.O.H.-G., 49113 to A.D., 99333 to C.T., and 128566 to A.D. and C.L.T.; Scholarship 1955 Curriculum vitae único number 204479 to J.C.C.; and Dirección General de Asuntos del Personal Académico/Universidad Nacional Autónoma de México IN211809 to A.D. and IN204109 to C.L.T.
[2]Correspondence: Claudia L. Treviño, Department of Developmental Genetics and Molecular Physiology, Biotechnology Institute, UNAM, Cuernavaca 62210, Mexico. FAX: 52 777 317 2388;
e-mail: ctrevino@ibt.unam.mx

Received: 14 June 2011.
First decision: 10 July 2011.
Accepted: 12 September 2011.

eISSN: 1529-7268 http://www.biolreprod.org
ISSN: 0006-3363

most likely regulates other Cl^- transporters during capacitation, as it occurs in other tissues (kidney, intestine, pancreas, and epididymis cells), where, for instance, a direct interaction between CFTR and Cl^- anion exchangers from the SLC26 family has been reported [13–16]. Specifically, SLC26A3 and SLC26A6 interact with CFTR through the regulatory (R) domain of CFTR and the sulfate transporter and anti-sigma (STAS) domain of SLC26 [10, 17]. The interaction requires the phosphorylation (via PKA) of both domains [18]. In addition to the R and STAS domains, CFTR and SLC26 transporters can interact via PDZ domain containing proteins or scaffolding proteins, such as SLC9A3R1 and SLC9A3R2 (Na^+/H^+ exchanger regulatory factor) [19–21], which contain two PDZ domains, allowing simultaneous interactions with multiple binding proteins forming large protein complexes underneath the plasma membrane [22].

Recently, SLC26A3 was detected in guinea pig sperm, where it appears to play an important role during sperm capacitation, in association with CFTR. The authors proposed that CFTR mediates HCO_3^- entry into spermatozoa by working in parallel with SLC26A3 and providing a recycling pathway for Cl^-. Moreover, considering the fact that a number of sperm functions, including motility, hyperactivation, capacitation, and AR, depend on HCO_3^- and Cl^-, SLC26A3 and CFTR may regulate diverse guinea pig sperm functions [7, 23]. Considering the latter, in this work we confirm the presence of SLC26A3 in mouse sperm, and show that this protein interacts with SLC26A6 and with SLC9A3R1. In addition, our results suggest that these proteins interact with CFTR and regulate the $[Cl^-]_i$ increase, the Em, and the pH_i changes observed in mouse sperm capacitation.

In this study, we found that SLC26A3, SLC26A6, and SLC9A3R1 are present in the mouse sperm midpiece, where CFTR is located [10]. Our findings also indicate that SLC26A3, SLC26A6, CFTR, and SLC9A3R1 coimmunoprecipitate and colocalize in mouse sperm. We also show that SLC26A3 participates in the $[Cl^-]_i$ increase and capacitation-associated hyperpolarization. CFTR is also involved in these events, as already reported [10]. Finally, our findings are consistent with the participation of SLC26A3, SLC26A6, and CFTR in the pH_i increase that takes place during capacitation. These results suggest that SLC26A3, SLC26A6, and CFTR are important for mouse sperm capacitation.

MATERIALS AND METHODS

Materials

TRIzol reagent, dibutyryl cAMP (db-cAMP), 3-isobutyl-1-methylxantine (IBMX), carbonyl cyanide *m*-chlorophenylhydrazone (CCCP), valinomycin, digitonin, 5-[(4-carboxyphenyl) methylene]-2-thioxo-3-[(3-trifluoromethyl) phenyl-4 thiazolidinone (inh-172) and polyclonal antibody against SLC9A3R1 (catalog no. N-7286) were purchased from Sigma (St. Louis, MO). N-[ethoxycarbonylmethyl]-6-methoxy-quinolinium bromide (MQAE), 3, 3′-dipropyl-thiadicarbocyanine iodide ($DiSC_3(5)$) and secondary antibodies (Alexa Fluor donkey anti-goat IgG [H + L] 647 and 488) were obtained from Invitrogen (Carlsbad, CA). 2′, 7′-bis-(2-carboxyethyl)-5-(and-6)-carboxyfluorescein (BCECF) was obtained from Molecular Probes (Eugene, OR). Polyclonal antibodies against SLC26A3 (catalog no. sc-34939), SLC26A6 (catalog no. sc-26728) and CFTR (catalog no. sc-8909) were purchased from Santa Cruz Biotechnology (Santa Cruz, CA). 1,2-Dioctanoyl-sn-glycerol (DOG) and phorbol 12-myristate 13-acetate (PMA) were purchased from Calbiochem (San Diego, CA). Tenidap (Tdap) and UK-5099 (5099) were kindly provided by Pfizer Inc. (Groton, CT).

MQAE, $DiSC_3(5)$, BCECF, CCCP, and valinomycin were prepared in dimethyl sulfoxide (DMSO) and stored at −20°C until use.

The db-cAMP (1 mM) and IBMX (100 μM) were prepared on the day of the experiment using Whitten Hepes-buffered medium (100 mM NaCl, 4.7 mM KCl, 1.2 mM KH_2PO_4, 1.2 mM $MgSO_4$, 5.4 mM dextrose, 0.8 mM pyruvic acid, 4.8 mM calcium L-lactate, 20 Hepes).

Sperm Preparation

Cauda epididymal mouse sperm were collected from CD1 retired male breeders. The animals were killed using protocols approved by the local Animal Care and Bioethics Committee of the Instituto de Biotecnología—Universidad Nacional Autónoma de México (this study was specifically approved by the Bioethics Committee [no. 94-2008/2010]). Minced cauda epididymides from each animal were placed in Whitten Hepes-buffered medium. This medium does not support capacitation unless supplemented with 5 mg/ml bovine serum albumin (BSA) and 24 mM $NaHCO_3$. After 10 min, the sperm suspension was washed in 10 ml of the same medium by centrifugation at $300 \times g$ for 5 min at room temperature. Sperm were diluted to a final concentration of 2×10^7 cells/ml in the appropriate medium according to the experiment. In all cases, pH was maintained at 7.4.

RNA Isolation and RT-PCR Experiments

Mouse pachytene, round, and elongated spermatids were isolated from testes [24]. Briefly, the testes were decapsulated and subjected to enzymatic digestion (collagenase/trypsin). The cell suspension was sedimented at unit gravity using a 2%–4% BSA/enriched Krebs-Ringer bicarbonate (EKRB; 120 mM NaCl, 25.2 mM $NaHCO_3$, 4.8 mM KCl, 1.2 mM KH_2PO_4, 1.2 mM $MgSO_4$, 1.3 mM $CaCl_2$, and 11 mM glucose) linear gradient. After sedimentation, 10-ml fractions were collected and cell identity was determined by bright-field microscopy according to size and shape and similar fractions were pooled. Total RNA was prepared from isolated pachytene, round, and elongated spermatids [25] using TRIzol Reagent according to the manufacturer's instructions. Complimentary DNA was synthesized from total RNA samples with random hexamer-primed reverse transcription (Superscript II RNase H-reverse transcriptase; Invitrogen). Complimentary DNA was then subjected to PCR amplification using TaqDNA polymerase (Invitrogen). SLC26A3, SLC26A6, and SLC9A3R1 primers were designed using the mouse reported nucleotide sequence for these genes (see Table 1). PCR programs included 35 cycles of amplification (94°C for 1 min, 55°C for 1 min, and 72°C for 30 sec, and a final extension at 72°C for 5 min). The absence of genomic DNA contamination in the RNA samples was confirmed with reverse transcription-negative controls (reverse transcription enzyme was omitted) for each experiment. Amplified products were analyzed by DNA sequencing in order to confirm their identity.

Sperm Membrane Purification

The preparation of sperm fractions was carried out as described previously [8]. Briefly, sperm (20×10^7 cells) were homogenized using 10 strokes with a Teflon Dounce homogenizer in Tris-HCl/EDTA buffer (50 mM Tris-HCl [pH 7.5], 1 mM EDTA) supplemented with protease inhibitors (protease inhibitor mixture; Roche Applied Science, Mannheim, Germany) plus 0.4 mM leupeptin, 0.4 mM aprotinin, 0.1 mM pepstatin, 300 mM benzamidine, and 0.32 mg/ml calpain I and II inhibitor. After homogenization, the sample was sonicated three times for 15 sec on ice at intervals of 1 min. Cell debris was pelleted ($1000 \times g$ for 10 min at 4°C), and the supernatant was centrifuged at $10\,000 \times g$ for 10 min at 4°C. The resultant pellet was discarded, and the supernatant was centrifuged at $100\,000 \times g$ for 1 h at 4°C. The final pellet, which contained the membrane fraction, was resuspended in sample buffer (10% SDS, 50% glycerol, 8 mM EDTA, 500 mM Trizma-base, pH 6.8) and used for SDS-PAGE and immunoblotting.

SDS-PAGE and Immunoblotting

Sperm membrane extracts were resuspended in sample buffer containing protease inhibitors without β-mercaptoethanol, and boiled for 5 min. Sperm samples were centrifuged at $10\,000 \times g$ for 15 min. After centrifugation, the supernatants were collected and β-mercaptoethanol was added to a final concentration of 5% (v/v). The samples were boiled for an additional 5 min and then subjected to SDS-PAGE 7 on 10% polyacrylamide gels. Electrotransfer of proteins to Immobilon P (Bio-Rad, Hercules, CA), and immunodetection was carried out as previously described [26]. Immunoblots were incubated with anti-SLC26A3 (1:100), anti-SLC26A6 (1:100), anti-CFTR (1:500), and anti-SLC9A3R1 (1:500) and developed with the appropriate (see below) secondary antibody (1:10 000) conjugated to horseradish peroxidase (HRP) (Zymed, San Francisco, CA) and the chemoluminescent ECL kit (Thermo Scientific, Waltham, MA) according to the manufacturer's instructions. Since the molecular weight of SLC9A3R1 is around 55 kDa, a secondary antibody that detects heavy chains, the molecular weight of which is also 55 kDa, could not be used. Therefore, for SLC9A3R1 detection, we used the following secondary antibody: HRP conjugate IgG fraction monoclonal mouse anti-rabbit IgG, light chain specific (catalog no. 211-032-171; Jackson Immunoresearch, West

TABLE 1. Sets of primers designed to amplify SLC26 members and SLC9A3R1 from mouse spermatogenic cells.

Gene	Forward primer 5′-3′	Reverse primer 5′-3′	At (°C)[a]	Predicted size (bp)	Genbank accession no.
Slc26a3	TACAGCGACCCATTCT	CCTTCAGGCTCATACAC	50	893	NM_021353.2
Slc26a6	TATCCTGTGCGTGAA	AATGAGCGTGAGTAGTT	52	657	NM_134420.4
Slc9a3r1	TTTATCCGTCTGGTAGAA CC	GGCTTAGACTTGTCGCTGT	56	398	NM_012030.2

[a] At, annealing temperature.

Grove, PA). All other proteins were detected using HRP conjugate rabbit anti-goat IgG (H + L) (Invitrogen; catalog no. 81-1620).

Indirect Immunofluorescence

Spermatozoa, collected as described above, were washed in PBS medium. After washing, sperm were resuspended in fixing solution (4% paraformaldehyde final concentration in PBS) and placed onto slides. Cells were allowed to settle for 30 min at room temperature in a humid chamber and washed (three times for 5 min) with PBS. After washes, cells were permeabilized in PBS-Triton X-100 (0.1% final concentration) for 10 min at room temperature in a humid chamber, and washed (three times for 5 min) with PBS. Slides were removed from the humid chamber and allowed to air dry. The sperm preparation was blocked with 5 % BSA for at least 2 h. Specific primary antibodies for SLC26A3 (1:20), SLC26A6 (1:20), CFTR (1:100), and SLC9A3R1 (1:100) were added to sperm samples and incubated overnight at 4°C. These samples were washed (3×5 min) with PBS, and then incubated with the appropriate secondary antibody (1:10 000) (Alexa-488) for 1 h at 37°C followed by three 5-min washes with PBS. In the case of double immunofluorescence experiments, the first primary antibodies were incubated overnight at 4°C. The samples were washed (three 5-min washes with PBS) and incubated with the secondary antibodies (Alexa-594) for 1 h at room temperature. Then, the second primary antibodies were added and incubated overnight. The samples were again washed (three 5-min washes with PBS) and incubated with secondary antibodies (Alexa-488 or Cy5) for 1 h at room temperature. Finally, the samples were washed three times for 5 min with PBS and mounted in PBS-glycerol or gelvatol, and examined using a confocal unit (Zeiss LSM510 META with a Zeiss Axiovert 200 M inverted microscope) with a 60× objective. Peptide competition control experiments were performed preincubating the antibody with its corresponding antigenic peptide for 1 h at room temperature, and the samples were then processed equally. The peptide for SLC9A3R1 antibody was not available; the control experiment was performed incubating only with the secondary antibody. In the case of double immunofluorescence experiments, the peptide competition controls were made separately.

Immunoprecipitation Assay

Sperm membrane proteins (50–60 μg) were resuspended in RIPA buffer (50 mM Tris [pH 7.4], 150 mM NaCl, 10% glycerol, 0.1% SDS, 1% Triton X-100, protease inhibitors cocktail [Roche], 10 mM NaF, 1 mM Na Vanadate, and 50 mM β-glycerophosphate) and then mixed with 5–10 μg of anti-SLC26A3, anti-SLC26A6, anti-CFTR, or anti-SLC9A3R1. This mixture was incubated for 2–4 h, maintaining the sample in a rocking platform at 4°C. Subsequently, 25 μg of protein G-sepharose (Pharmacia Biotech, Uppsala, Sweden) were added, and the mixture was incubated overnight on a rocking platform at 4°C. The sample was centrifuged at 1000 rpm for 1 min, the supernatant recovered and washed by centrifugation three times with PBS-Triton X-100 (0.1%) and three times with PBS. The immunoprecipitated samples were eluted by adding 100 μl of glycine-HCl buffer (0.1 M glycine [pH 2.5]), stirred for 60 sec, and centrifuged at 1000 rpm for 1 min. The supernatant was mixed with 25 μl of trizma-base 1 M. The resulting sample was loaded onto SDS-PAGE 7 on 10% polyacrylamide gels.

Intracellular Cl^- Measurements in Sperm Populations

The $[Cl^-]_i$ was measured in sperm populations using MQAE, a Cl^--sensitive fluorescent dye, as previously described [10]. Briefly, sperm were incubated with 10 mM MQAE for 30 min at 37°C. Excess MQAE was removed by diluting sperm with Whitten medium and centrifuging for 3 min at $300 \times g$. The sperm pellet was resuspended in aliquots of 4×10^6 sperm/ml in the same medium. The influence of different drugs on $[Cl^-]_i$ was determined using sperm suspensions loaded with MQAE after recording the basal fluorescence (350/460 nm excitation/emission) for 1–3 min, and measuring for a further 5–10 min after the addition of the drug. Two controls were performed: 1) drug solvents (DMSO or water) were added while the fluorescence was recorded; and 2) MQAE fluorescence without cells was recorded, and the drugs were added. No significant fluorescence changes were observed after performing both controls. The sperm $[Cl^-]_i$ was calibrated according to Garcia and Meizel [27]. Briefly, mouse sperm were incubated for 30 min in Whitten Hepes-buffered medium containing different Cl^- concentrations (0–100 mM) and 10 mM MQAE. Excess MQAE was removed as described above, and emission fluorescence intensity data from sperm suspensions (2×10^6 sperm/ml) were recorded for 120 sec. The intracellular and extracellular $[Cl^-]$ were equilibrated by permeabilizing the sperm membrane with digitonin (10 μM), and the fluorescence was recorded for another 120 sec. The $[Cl^-]_i$ was calculated as described previously [27].

Membrane Potential Assay in Sperm Populations

Em was measured as previously described [5]. Briefly, sperm were collected as previously indicated, and diluted in the appropriate medium. Spermatozoa were incubated in complete Whitten Hepes-buffered medium (supplemented with BSA and $NaHCO_3$) for 10 and 60 min for noncapacitated and capacitated condition, respectively. The 10-min incubation for the noncapacitated condition does not promote the capacitation-associated hyperpolarization (clearly observed after 60-min incubation). At 8 min before the measurement, $DiSC_3(5)$ (1 μM final) was added to the sperm suspension and the mixture was further incubated for 5 min at 37°C. Afterwards, CCCP (1 μM final) was added to induce the collapse of the mitochondrial potential, and sperm suspension was incubated for an additional 3 min. After this period, 800 μl of the suspension were transferred to a gently stirred cuvette at 37°C, and the fluorescence (640/670 nm excitation/emission) was recorded continuously. Calibration was performed as described previously [5] by adding 1 μM valinomycin and sequential additions of KCl.

Intracellular pH Measurements in Sperm Populations

The pH_i was measured using the pH-sensitive fluorescent dye BCECF (0.5 μM) in spermatozoa (collected as previously indicated). Cells were incubated with the dye for 15 min at 37°C. Excess BCECF was removed by diluting sperm with Whitten Hepes-buffered medium and centrifuging for 3 min at $300 \times g$. The sperm pellet was resuspended in the same medium to obtain a concentration of 4×10^6 sperm/ml. The effect of different drugs on pH_i was determined using sperm suspensions loaded with BCECF incubated during 10 min (noncapacitated) or 60 min (capacitated) in complete Whitten Hepes-buffered medium (supplemented with BSA and $NaHCO_3$). We recorded the fluorescence (510/450 nm for excitation and 550 nm for emission) for 1 min. The short incubation period for the noncapacitated condition does not promote the capacitation-associated hyperpolarization, but provides equal experimental conditions. Calibration was performed as described previously [28], adding 0.12% Triton X-100 and subsequent HCl additions (0.1%). The addition of Triton X-100 increased the fluorescence ratio to a value corresponding to the pH of Whitten Hepes-buffered medium. Three consecutive aliquots of HCl were then added to the cuvette, which resulted in step-wise decreases in fluorescence ratios. At each step (including the one reached after Triton addition), the pH was determined with a conventional pH electrode. The BCECF ratio values were converted to pH_i with the software FeliX version 1.41 (Photon Technology International, Birmingham, NJ).

Statistical Analysis

The data are expressed as the mean ± SEM. Statistical analysis was performed using the Wilcoxon (Mann-Whitney) nonparametric test for unpaired and paired data.

RESULTS

SLC26A3, SLC26A6, and SLC9A3R1 Are Present in Mouse Sperm

Previous reports have shown that the activation of CFTR is required for sperm capacitation [9, 10]; however, its opening

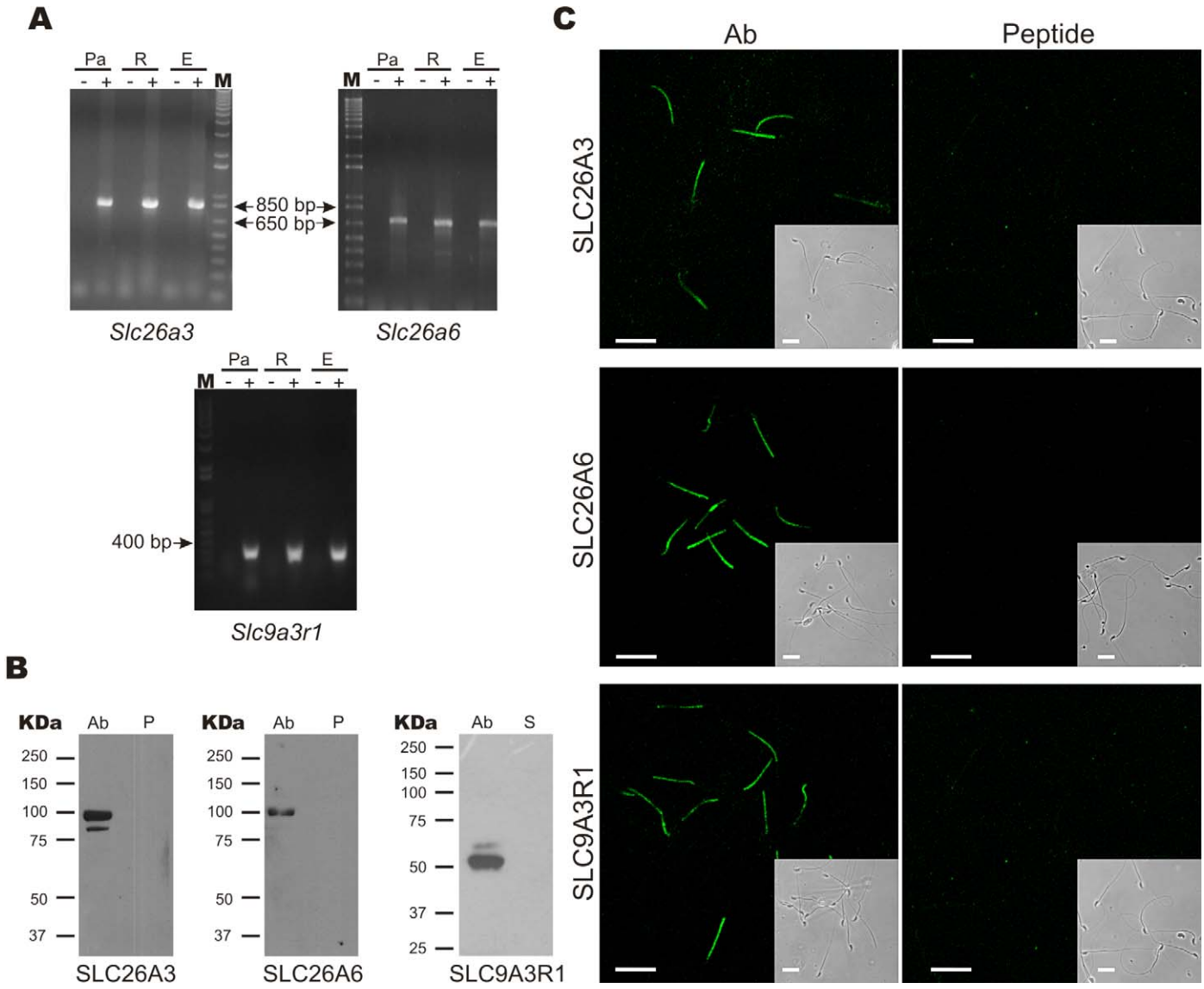

FIG. 1. SLC26A3, SLC26A6, and SLC9A3R1 are localized in the mouse sperm midpiece. **A**) RT-PCR showing transcripts for SLC26A3, SLC26A6, and SLC9A3R1 from mouse spermatogenic cells: Pachytene (Pa), round (R), and elongated cells (E), in the presence (+) or absence (–) of reverse transcriptase; the size of the molecular weight markers (M) is indicated in base pairs (bp). **B**) Western blot experiments using sperm membrane extracts to detect SLC26A3, SLC26A6, and SLC9A3R1. The left lane (Ab) shows the signal with the antibody; the right lane corresponds to samples preincubated with the corresponding antigenic peptide (P) or with the secondary (S) antibody only. The molecular weight markers in kiloDaltons (kDa) are shown to the left of each panel. Expected size: 98, 95, and 55 kDa for SLC26A3, SLC26A6, and SLC9A3R1, respectively. **C**) Immunocytochemistry experiments for SLC26A3, SLC26A6, and SLC9A3R1; left panels show staining with the indicated Ab, and right panels show signal competition by preincubation of the primary antibody with the corresponding antigenic peptide. In the case of SLC9A3R1, the control experiment was performed incubating with the secondary antibody only (peptide is not available). All proteins localize to the sperm midpiece. The insets in each panel show the corresponding phase-contrast image. Bar = 20 μm. The images are representative of four independent experiments.

cannot explain the $[Cl^-]_i$ increase observed during this process, which suggests that other transporters could be involved [10]. In tissues like pancreas, epididymis, and intestine, CFTR and at least two members of the SLC26 family, SLC26A3 and SLC26A6, have been shown to interact [13–16]. Therefore, we investigated whether these proteins were present in mouse spermatozoa and if they interacted.

First, RT-PCR using specific primers for SLC26A3, SLC26A6, and SLC9A3R1 revealed transcript fragments of the expected length in spermatogenic cells (SLC26A3, 893 bp; SLC26A6, 657 bp; and SLC9A3R1, 398 bp) (Fig. 1A). Their identities were confirmed by DNA sequencing. In addition, these proteins were detected in purified sperm membranes by Western blot (Fig. 1B). The protein bands had the expected molecular weights for SLC26A3 (98 kDa), SLC26A6 (95 kDa), and SLC9A3R1 (55 kDa) (Fig. 1B). Moreover, preincubation of SLC26A3 and SLC26A6 antibodies with the corresponding antigenic peptide eliminated the signal (Fig. 1B). In the case of SLC9A3R1, although the antigenic peptide was not available, secondary antibody alone served as negative control (Fig. 1B). Using immunofluorescence, these validated antibodies localized SLC26A3, SLC26A6, and SLC9A3R1 in the sperm midpiece (Fig. 1C).

SLC26A3, SLC26A6, and SLC9A3R1 Colocalize and Interact with CFTR in Mouse Sperm

In a previous report, we found that, similar to SLC26A3, SLC26A6, and SLC9A3R1, CFTR also localized to the

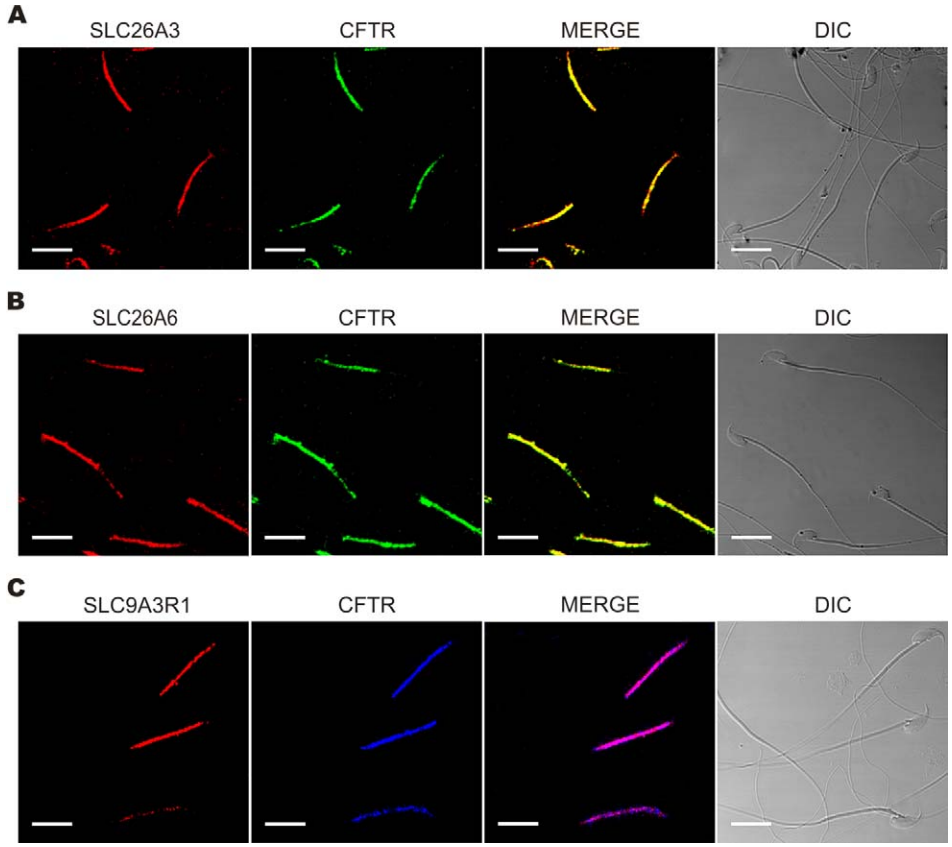

FIG. 2. SLC26A3, SLC26A6, and SLC9A3R1 colocalize with CFTR. Swim-up-separated sperm were fixed, permeabilized, and exposed to anti-SLC26A3 (**A**), anti-SLC26A6 (**B**), and anti-SLC9A3R1 (**C**) (red signal); the same cells were also exposed to anti-CFTR (green or blue signal). The merged and phase-contrast images are also shown (DIC). Bar = 20 μm. Images are representative of four independent experiments.

midpiece of mouse spermatozoa [10]. Immunofluorescence experiments were designed to determine the colocalization of each of the new proteins reported here with CFTR. We found that SLC26A3 (Fig. 2A), SLC26A6 (Fig. 2B), and SLC9A3R1 (Fig. 2C) colocalize with CFTR, suggesting that these proteins may interact and participate in the regulation of the Cl^-/HCO_3^- concentration in spermatozoa, as observed in other tissues [16, 17, 19, 29, 30].

CFTR interacts and positively regulates the activity of SLC26A3 and SLC26A6 in many tissues, such as intestines [13, 30], pancreas [15, 29], and epididymis [16, 31]. This regulation is mediated by PDZ domain containing proteins [20, 32]. Since we found that all these proteins colocalize in spermatozoa, we next investigated whether the same type of interaction occurs in sperm. To this end, we performed reciprocal immunoprecipitation experiments using purified sperm membranes and antibodies to SLC26A3, SLC26A6, CFTR, or SLC9A3R1, and blotted against SLC26A3, SLC26A6, SLC9A3R1, or CFTR (Fig. 3, A–D, respectively). We confirmed the interaction of these four proteins in all experimental conditions. The targeted protein was always detected in the eluted fraction except, as expected, in the negative control in which an unrelated antibody (anti-pyruvate dehydrogenase E1β chain, PDHE1β) was used for immunoprecipitation. Moreover, we did additional controls to ensure the specificity of our detection (Supplemental Fig. S1; all Supplemental Data are available online at www.biolreprod.org).

Slc26A3 and CFTR Are Involved in the $[Cl^-]_i$ Increase Induced by db-cAMP in Noncapacitated Sperm

Previously, our group reported that the addition of db-cAMP in noncapacitated mouse sperm elevated the $[Cl^-]_i$; this increase was inhibited by diphenylamine 2-carboxylate (DPC), a CFTR antagonist [10]. This finding supported the notion that CFTR is involved in $[Cl^-]_i$ increase during sperm capacitation. Taking into consideration that SLC26A3 and SLC26A6 are present in spermatozoa and interact with CFTR, we explored whether these exchangers were involved in this $[Cl^-]_i$ increase. Figure 4A shows that addition of 1 mM db-cAMP (a permeable analogue of cAMP) to noncapacitated sperm in the presence of 100 μM IBMX (a phosphodiesterase inhibitor) increased their $[Cl^-]_i$ by approximately 10 mM (25–35 mM). This increase was inhibited 50% by two SLC26A3 antagonists (Tdap and 5099) with estimated half-maximal inhibitory concentration values for Tdap and 5099 of 2.9 and 2.8 μM, respectively (Fig. 4B), similar to those described for these inhibitors [33]. The CFTR inhibitor, inh-172 (Fig. 4D), also eliminated 50% of the db-cAMP-stimulated $[Cl^-]_i$ increase (estimated $IC_{50} = 90$ nM), supporting previous results using DPC as CFTR inhibitor [10]. In contrast, inhibitors of SLC26A6 (DOG and PMA) did not affect the $[Cl^-]_i$ increase stimulated by db-cAMP (Fig. 4C). It is worth mentioning that DOG and PMA inhibit SLC26A6 indirectly [34] through the activation of PKC [35]. Together, these results suggest that SLC26A3 and CFTR, but not PKC and/or SLC26A6, participate in regulating the $[Cl^-]_i$ during capacitation.

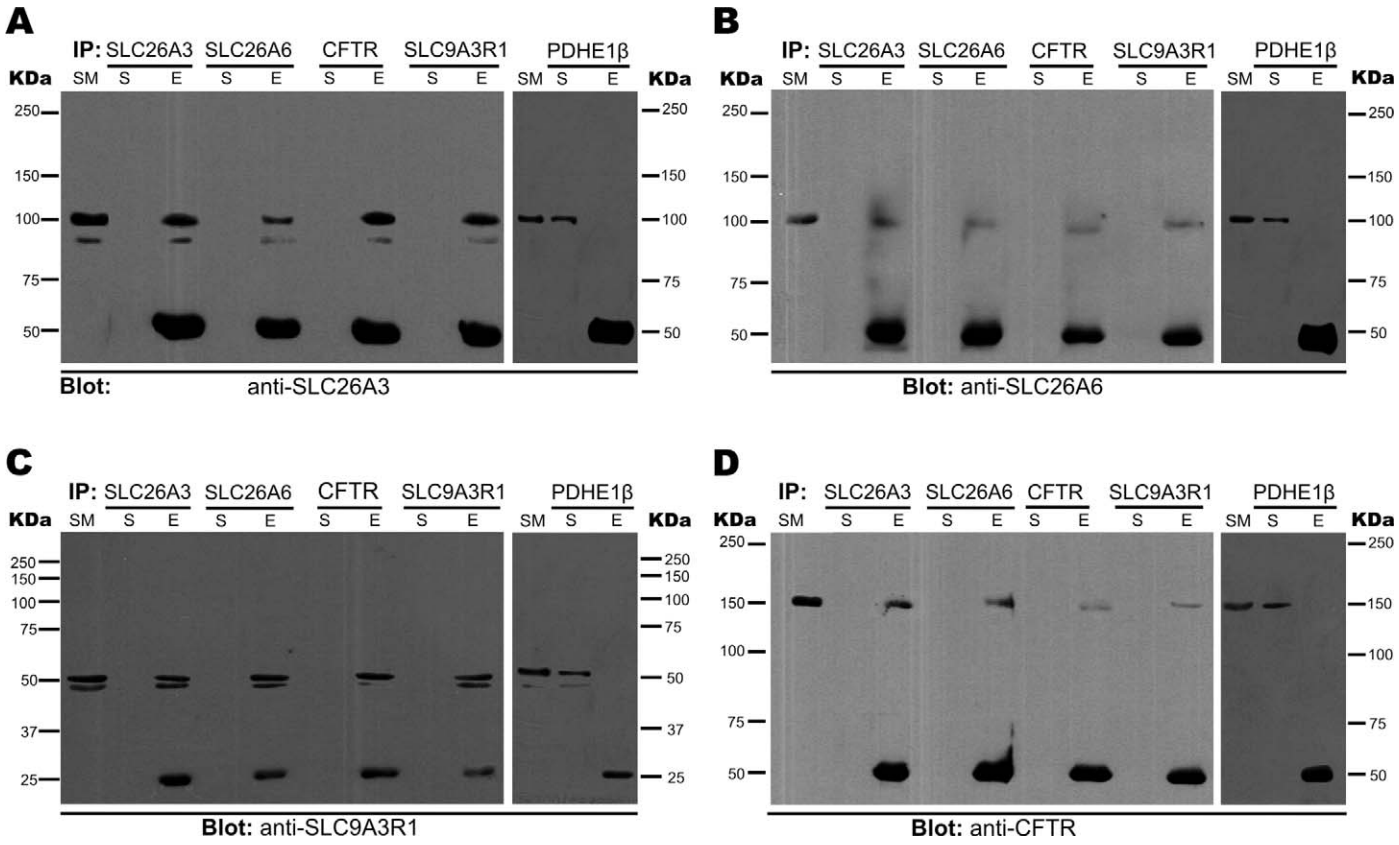

FIG. 3. SLC26A3, SLC26A6, and SLC9A3R1 interact with CFTR in mouse sperm. Purified sperm membranes were used to immunoprecipitate SLC26A3, SLC26A6, CFTR, and SLC9A3R1. The input (SM), the supernatant (S), and the eluted fraction (E) were loaded in 7% acrylamide gels, blotted, and probed by Western blot assays with anti-SLC26A3 (**A**), anti-SLC26A6 (**B**), anti-SLC9A3R1 (**C**), and anti-CFTR (**D**). Molecular weight markers (in kDa) are shown on both sides of each panel. An immunoprecipitation negative control was performed in each case using PDHE1β (shown at the right of each panel). Expected sizes: 98, 95, 55, 165, and 37 kDa for SLC26A3, SLC26A6, SLC9A3R1, CFTR, and PDHE1β, respectively. The 50-kDa band in blots for SLC26A3, SLC26A6, and CFTR and the 25-kDa band in the blot for SLC9A3R1 correspond to the light chains from IgGs, which were detected by the secondary antibody used in each case (goat and rabbit, respectively). These blots are representative of three independent experiments.

SLC26A3 and CFTR Are Involved in the Capacitation-Associated Hyperpolarization

Cl^- is an important element for the capacitation-associated hyperpolarization in mouse sperm, and CFTR contributes to this hyperpolarization [10]. In order to determine whether SLC26A3 and SLC26A6 are also involved in the capacitation-associated hyperpolarization, we measured Em using $DISC_3(5)$ dye in noncapacitated and capacitated spermatozoa in the presence or absence of SLC26A3, SLC26A6, and CFTR inhibitors (Fig. 5). To perform these experiments, noncapacitated spermatozoa were incubated in capacitating medium for only 10 min in order to ensure the same experimental conditions as for capacitated spermatozoa, but without the time required to promote hyperpolarization. As previously reported [36], Em hyperpolarizes during capacitation. We obtained an Em of −36 mV and −60 mV for noncapacitated and capacitated spermatozoa, respectively (Fig. 5A). Subsequently, spermatozoa were incubated with SLC26A3 inhibitors (Tdap and 5099) during capacitation; both antagonists (Tdap and 5099) inhibited the hyperpolarization by about 30%, with an estimated IC_{50} of 2.6 and 3.0 μM, respectively (Fig. 5B). Interestingly, CFTR inhibitor (inh-172) almost completely blocked hyperpolarization, with an estimated IC_{50} of 100 nM (Fig. 5D), which is in agreement with results previously reported [10], suggesting the participation of CFTR in the capacitation-associated hyperpolarization. Finally, we found that SLC26A6 inhibitors (DOG and PMA) did not affect the capacitation-associated hyperpolarization (Fig. 5C). These results are also consistent with the contention that SLC26A3 and CFTR, but not SLC26A6, contribute to the capacitation-associated hyperpolarization in mouse sperm.

The addition of HCO_3^- to noncapacitated spermatozoa induces Em hyperpolarization, a response that is Na^+ dependent [5]. These results are consistent with the involvement of an NBC in HCO_3^- entry into the cell. However, the presence of an NBC does not exclude the participation of other transporters, a possibility consistent with the inhibition caused by 4,4′-diisothio-cyanatostilbene-2,2′-disulfonic acid (DIDS) and 4-acetamido-4′-isothiocyanato-stilbene-2,2′-disulfonic acid (SITS) (~80% inhibition with both compounds), two broad-spectrum inhibitors of anionic transport [5]. To determine whether SLC26A3, SLC26A6, and/or CFTR mediate the HCO_3^--induced hyperpolarization, we measured the effect of SLC26A3, SLC26A6, and CFTR inhibitors in the HCO_3^--induced hyperpolarization. Figure 6A shows that HCO_3^- addition to noncapacitated spermatozoa induces a hyperpolarization of about 20 mV, as previously reported [5]. SLC26A3 inhibitors (Tdap and 5099) blocked ~50% of the HCO_3^--induced hyperpolarization (Fig. 6B), whereas DOG and PMA did not (Fig. 6C). Finally, the CFTR inhibitor inh-172 also blocked the HCO_3^--induced hyperpolarization by ~60% (Fig. 6D). Our results suggest that SLC26A3 and CFTR are also involved in the HCO_3^--induced hyperpolarization.

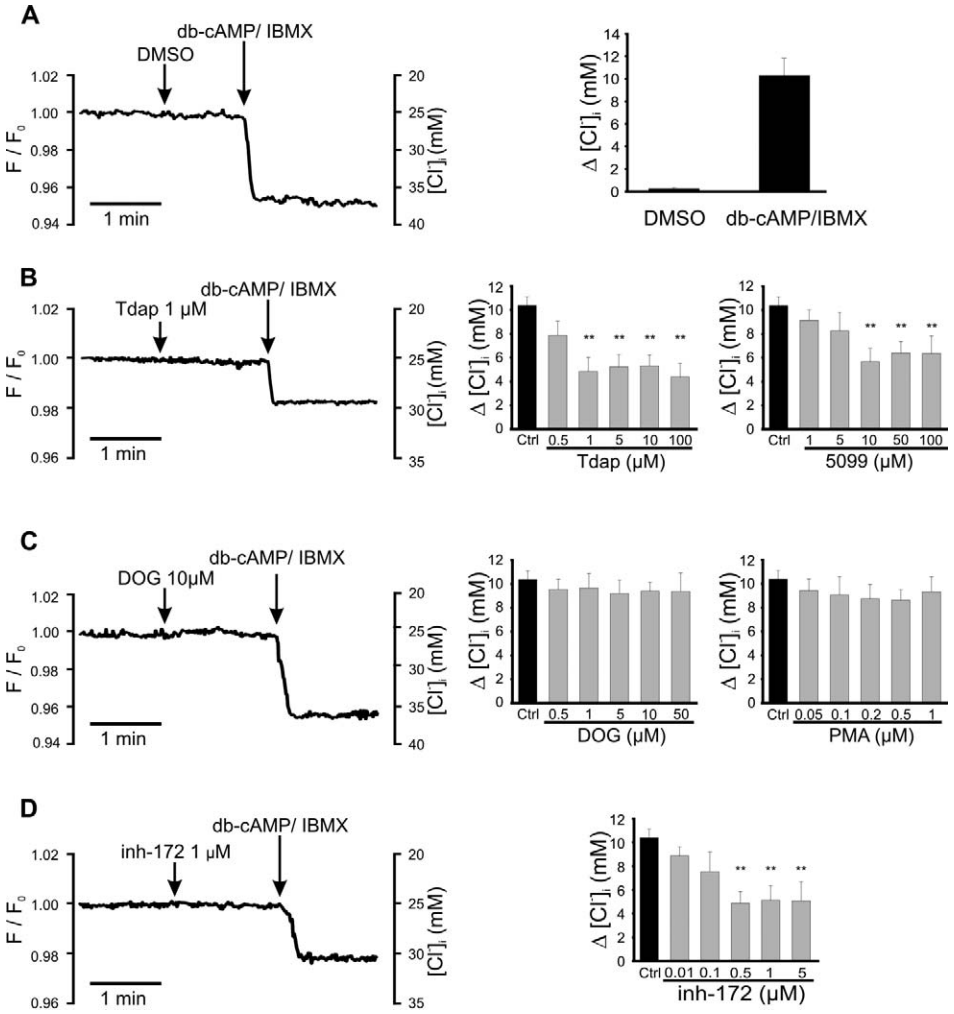

FIG. 4. Slc26A3 and CFTR are involved in the $[Cl^-]_i$ increase induced by db-cAMP in noncapacitated sperm. Intracellular Cl^- measurements with MQAE (10 mM) were performed in noncapacitated mouse spermatozoa. Addition of db-cAMP/IBMX increases $[Cl^-]_i$ (detected as a reduction in fluorescence), previous addition of solvent (DMSO) as negative control is also shown (**A**). The $[Cl^-]_i$ increase was partially blocked by SLC26A3 (Tdap and 5099) (**B**) and CFTR (inh-172) (**D**) inhibitors, but not by SLC26A6 inhibitors (DOG and PMA) (**C**). Left panels show representative fluorescent traces plotted as F/F_0 (left axis) vs. time. The right axis shows the corresponding $[Cl^-]_i$, calculated as described in *Materials and Methods*. Right panels summarize the change (Δ) in the $[Cl^-]_i$ in response to db-cAMP in the absence (black bars) or presence (gray bars) of different concentrations of the inhibitors used. Results are means ± SEM. N.S., $P > 0.05$; $^{**}P \leq 0.01$ (n = 4).

SLC26A3, SLC26A6, and CFTR Are Involved in the Capacitation-Associated pH_i Increase

In human [28, 37] and mouse [38] spermatozoa, pH_i increases during capacitation. The estimated increase in mouse sperm is approximately 6.4 to 6.8. HCO_3^- influx may contribute to this pH_i increase [38, 39]. SLC26A3, SLC26A6, and CFTR inhibitors were used to determine whether these transporters are involved in the pH_i increase associated with capacitation. The permeable fluorescent indicator BCECF was used to measure pH_i in mouse spermatozoa. Figure 7 shows that pH_i is 6.4 in noncapacitated spermatozoa and increases to 6.8 after 60 min of capacitation, in complete Whitten Hepes-buffered medium (containing BSA and $NaHCO_3$; black bars). Tdap and 5099 inhibited the capacitation-associated pH_i increase by 34%, with an estimated IC_{50} of 3.5 and 8 µM, respectively (Fig. 7A, gray bars). Unexpectedly, SLC26A6 antagonists also inhibited ~30% of the capacitation-associated pH_i increase (Fig. 7B), with IC_{50} values of 5 µM and 160 nM for DOG and PMA, respectively. Because SLC26A6 inhibition by these compounds is indirect, the interpretation of these results is complex (see *Discussion*). Finally, the CFTR inhibitor (inh-172) diminished the capacitation-associated pH_i increase by 36%, with an estimated IC_{50} of 240 nM (Fig. 7C). Figure 7D exemplifies the calibration method used for pH_i determination. These results are in accordance with the involvement of SLC26A3 and CFTR in the pH_i increase associated with mouse sperm capacitation.

DISCUSSION

It is well established that Cl^- and HCO_3^- play an essential role in sperm capacitation and are required for tyrosine phosphorylation, Em hyperpolarization, and the preparation for a physiologically induced AR [7, 8, 10, 40]. Experiments using specific CFTR inhibitors strongly suggest that this channel participates in the capacitation-associated hyperpolarization and the AR [9, 10], although its inhibition does not affect tyrosine phosphorylation [8, 41]. In many cell types, there are interrelationships between the transport of Cl^- and HCO_3^- [7, 8, 42]. It is important to consider that in mouse spermatozoa, Em_{Cl-} is close to the cell EM, so the opening of

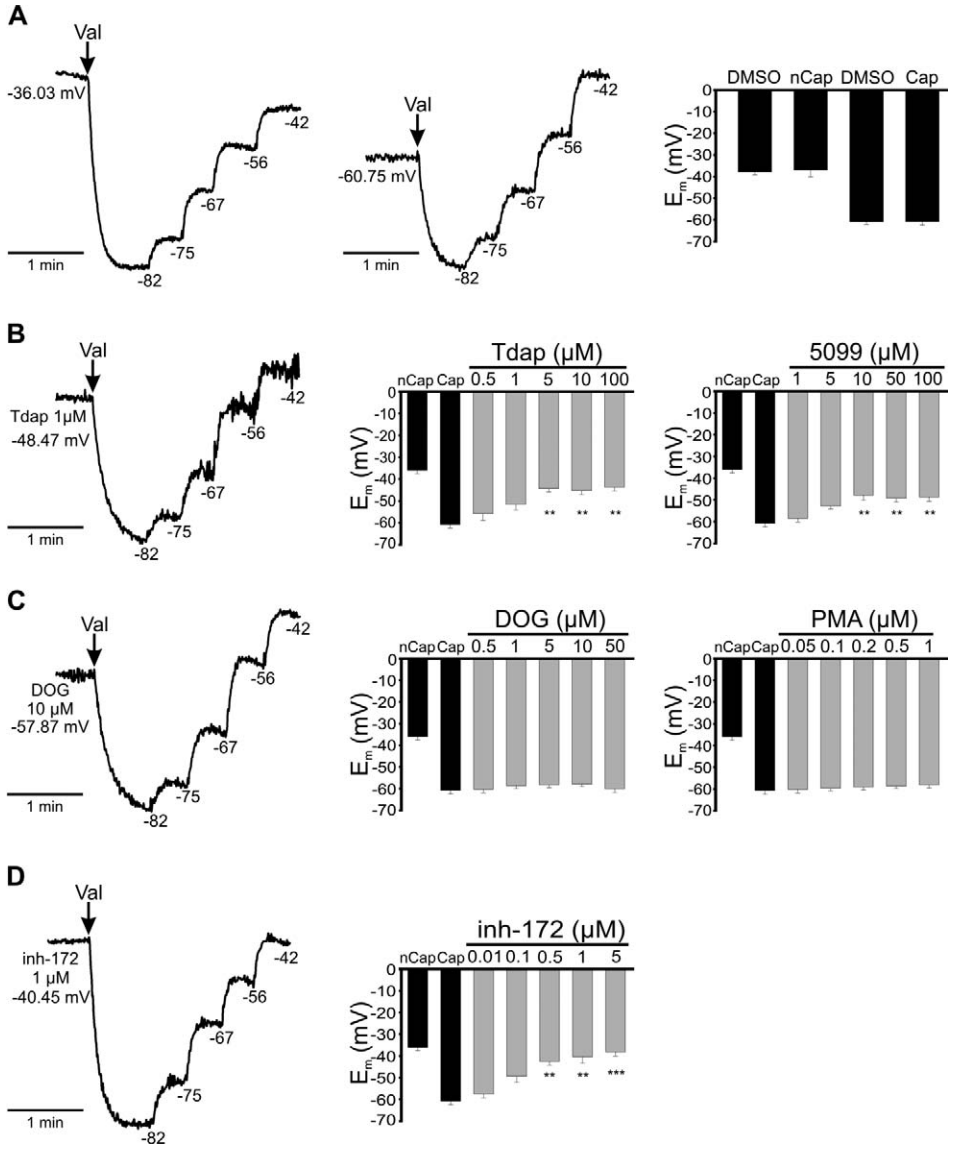

FIG. 5. SLC26A3 and CFTR are involved in the capacitation-associated hyperpolarization. Membrane potential measurements in mouse spermatozoa using $DISC_3(5)$ 1 μM, as described in *Materials and Methods*. The traces on the left in all panels are representative fluorescence traces with internal calibration using valinomycin (val) and subsequent KCl additions to determine the Em in each condition. The numbers to the right of each KCl addition correspond to the estimated theoretical potential using the Nerst equation. **A**) Representative traces from noncapacitated spermatozoa (nCap) (left), capacitated spermatozoa (Cap) (middle), and summary of the results (right). Representative traces (left) from capacitated sperm in the presence of Tdap (**B**), DOG (**C**), and inh-172 (**D**) at the indicated concentration. Summary of the sperm Em (right) in control conditions (black bars, noncapacitated [nCap] and capacitated [Cap]) or in the presence during capacitation of SLC26A3 (Tdap or 5099), SLC26A6 (DOG or PMA), or CFTR (inh-172) inhibitors (gray bars) at the indicated concentrations. Results are means ± SEM. N.S., $P > 0.05$; $^{**}P \leq 0.01$; $^{***}P \leq 0.001$ (n = 3).

any Cl^- channel would not result in a considerable Cl^- influx into the cell. Therefore, its increase during capacitation can only be explained by the participation of other Cl^- transporters. In guinea pig spermatozoa, it was recently reported that Cl^- and HCO_3^- are also essential for sperm capacitation, and that SLC26A3 and CFTR are present in this species [7]. However, in that paper, the authors report that CFTR was localized to the equatorial segment and SLC26A3 to the acrosome region, making it difficult to explain how these two proteins can physically interact, being located at different cellular regions. We tested our set of antibodies against CFTR, SLC26A3, and SLC26A6 in guinea pig sperm and obtained, as for mouse sperm, strong staining in the midpiece, although some faint staining can also be observed in the head; therefore, we cannot rule out that these proteins are also present in the head, as reported by Chen et al. [7] (data not shown). In kidney, pancreas, intestine, and epididymis, CFTR physically and functionally interacts with members of the SLC26 family—specifically, SLC26A3 and SLC26A6 [13–16]. Establishing colocalization is very important, since it has been recently demonstrated that the interactions among SLC26 transporters, and those with CFTR, are determinant for the type and direction of transport they perform [43, 44].

We found the presence of SLC26A3, SLC26A6, and SLC9A3R1 in membrane extracts of mouse sperm with Western blot experiments. It is important to point out that we observed some differences in the molecular weight of SLC26A3 and SLC26A6 compared with other reports. For example, some report a band 75 kDa for SLC26A3 [7, 33], and others found SLC26A3 with a size of 98 kDa [45]. In this

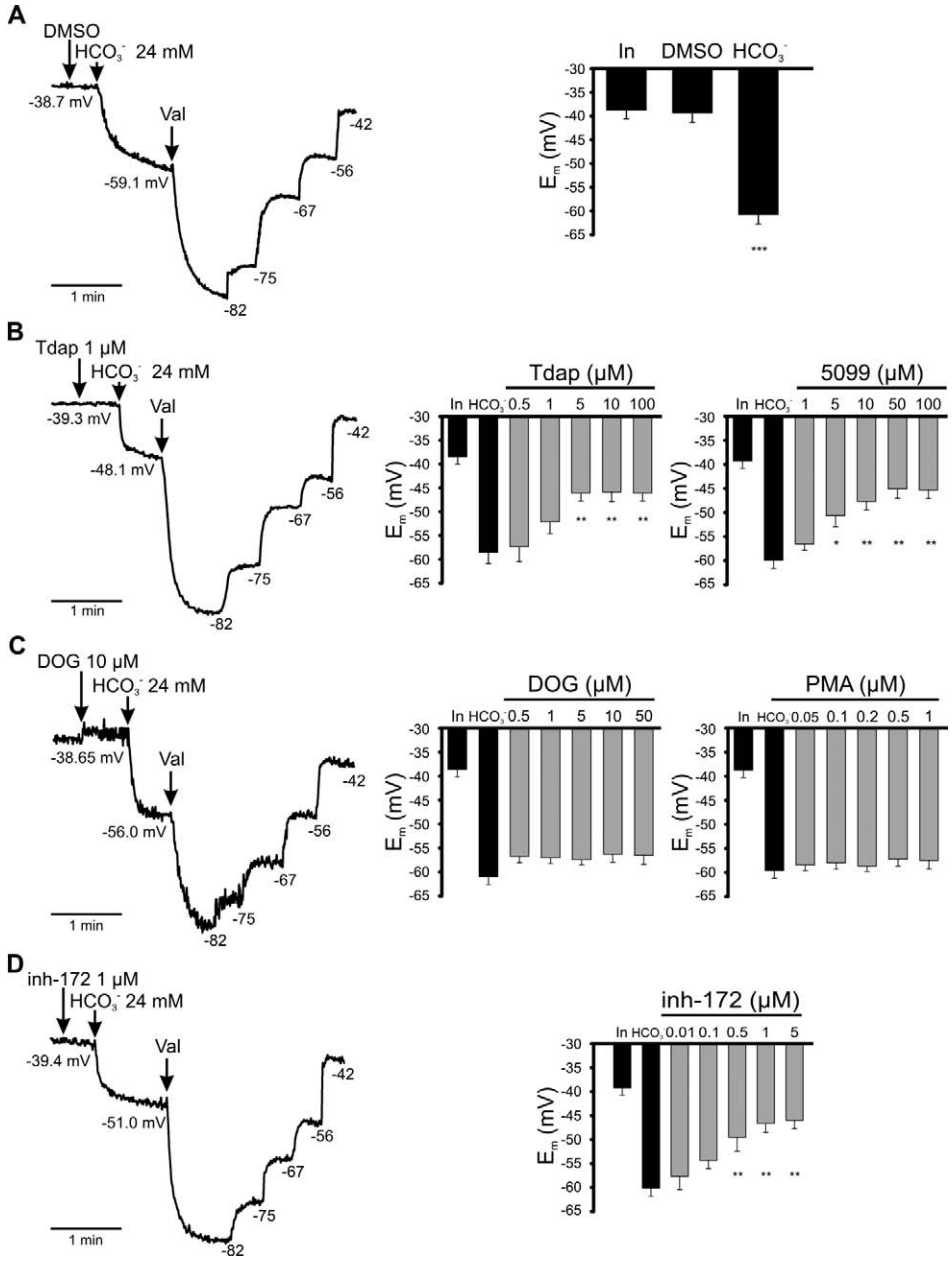

FIG. 6. SLC26A3 and CFTR are involved in the HCO_3^--induced hyperpolarization. Measurements of membrane potential using $DISC_3(5)$ in noncapacitated mouse spermatozoa. On the left are Representative fluorescent traces with internal calibration using valinomycin (val) and subsequent KCl additions to determine the Em obtained by HCO_3^- addition. The Em values (calculated with the internal calibration, right side of the trace) before and after the addition of HCO_3^- are indicated in each trace (arrows) in the presence of DMSO (**A**), Tdap (**B**), DOG (**C**), or inh-172 (**D**). On the right is a summary of the initial Em (In), the Em reached after the HCO_3^- addition (HCO_3^-) in the absence (black bars) or presence of SLC26A3 (Tdap and 5099), SLC26A6 (DOG and PMA) or CFTR (inh-172) inhibitors (gray bars) at the indicated concentrations. Results are means ± SEM. N.S., $P > 0.05$; *$P \leq 0.05$; **$P \leq 0.01$; ***$P \leq 0.001$ (n = 3).

work, we used antibodies from Santa Cruz Biotechnology. The data sheet shows a Western blot with two bands of about 90 and 120 kDa; we also obtained two bands of approximately the same weights. It is also important to consider that SLC26A3 undergoes posttranslational modifications, such as glycosylation, which can alter its molecular weight [46, 47]. With respect to the molecular weight of SLC26A6, there are reports showing that it has a size of between 80 and 85 kDa [48, 49]. The antibody data sheet from Santa Cruz Biotechnology shows a band of about 90 kDa. However, there are also reports of splice variants for SLC26A6 with varying molecular weights [48, 49]. Given that peptide competition experiments blocked the signal, we are confident that the band we obtained (100 kDa) corresponds to SLC26A6.

In this report, we show that SLC26A3 and SLC26A6 are present in the midpiece of mouse sperm, the same location reported for the CFTR channel [10], and that a PDZ-binding protein, SLC9A3R1, is also in the midpiece. These domains bind to the carboxyl termini of SLC26A3 and SLC26A6, and help to maintain their assembly with CFTR channels, forming a functional Cl^-/HCO_3^- transporter complex. The Cl^-/HCO_3^- transporter function is regulated through the STAS domain of SLC26 transporters and the R domain of the CFTR, with mutual enhancement of their transport activity [17, 18].

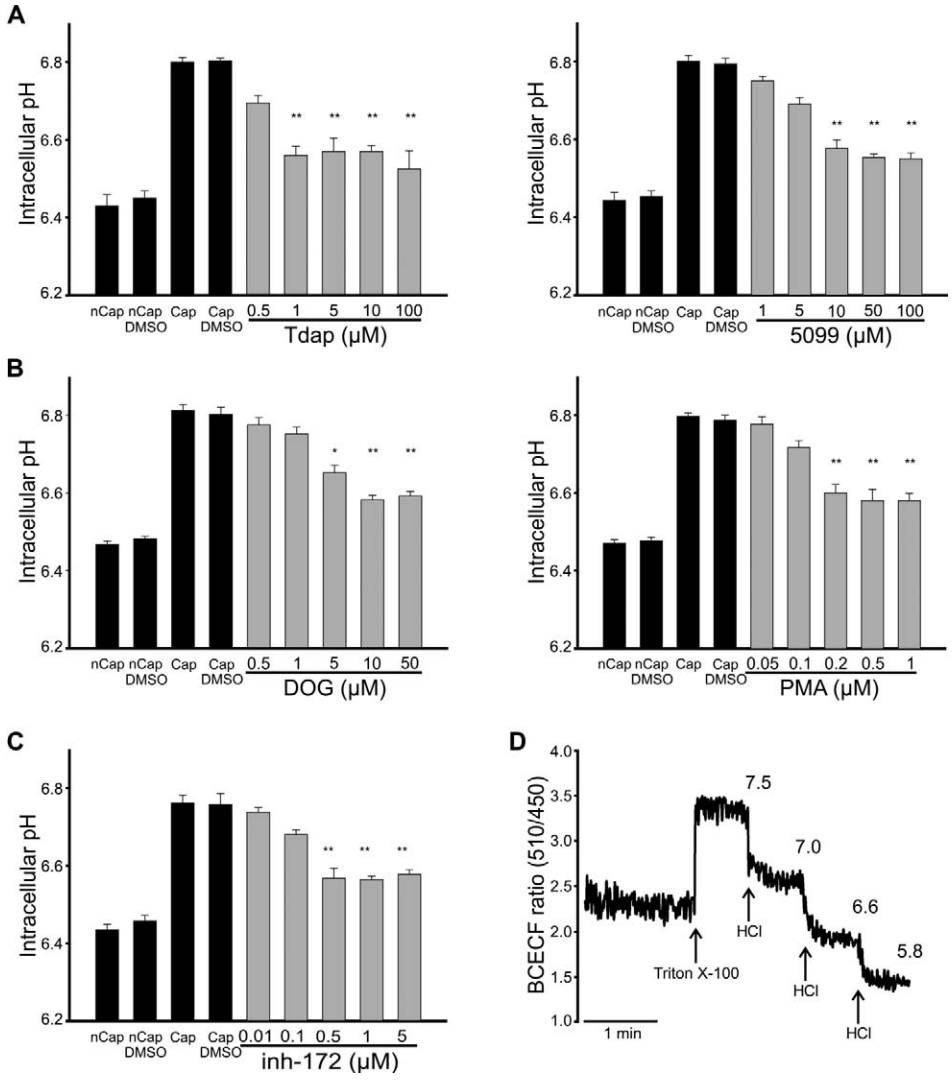

FIG. 7. SLC26A3, SLC26A6, and CFTR are involved in the capacitation-associated pH_i increase. Intracellular pH measurements in mouse spermatozoa using BCECF (0.5 μM), as described in *Materials and Methods*. Summary of the capacitation-induced pH_i changes in noncapacitated (nCap) and capacitated (Cap) control conditions (black bars) or in the presence (gray bars) during capacitation of Tdap/5099 (**A**), DOG/PMA (**B**), or inh-172 (**C**) at the indicated concentrations. **D**) Representative fluorescence trace that exemplifies the calibration used in each experiment. Below the trace, the Triton X-100 addition and the subsequent HCl additions (arrows) are indicated. Above the trace, the corresponding pH_e values measured using a conventional pH electrode are indicated. The BCECF fluorescence ratio (y axis) obtained in each trace was converted to pH_i using FeliX 1.41 software. Results are means ± SEM. N.S., $P > 0.05$; *$P \leq 0.05$; **$P \leq 0.01$ (n = 5).

Interestingly, we provide evidence for the physical interaction between SCL26A3, SLC26A6, SLC9A3R1, and CFTR in mouse sperm, suggesting that the regulatory mechanisms described in other cell types are preserved in spermatozoa.

To study the contribution of SLC26A3, SLC26A6, and CFTR in the events related to capacitation, $[Cl^-]_i$, Em, and pH_i were measured. Our results indicate that the dp-cAMP-induced $[Cl^-]_i$ increase and the capacitation-associated hyperpolarization were partially inhibited by the two SLC26A3 antagonists used here. Our Em results with the SLC26A3 inhibitors are consistent with the recently reported stoichiometry of two Cl^- inwards in exchange for one intracellular HCO_3^- [50, 51].

As expected from our previous work [10], the specific CFTR inhibitor, inh-172, also reduced the db-cAMP-induced increase in $[Cl^-]_i$ and the capacitation-associated hyperpolarization. However, the simultaneous inhibition of SLC26A3 and CFTR did not cause an additive effect on either the $[Cl^-]_i$ increase stimulated by db-cAMP or the capacitation-associated hyperpolarization (data not shown). These findings suggest that SLC26A3 and CFTR are part of a complex where, as previously reported [17, 18, 52], each transporter activity affects the other. Interestingly, inhibition of CFTR [8, 41] and SLC26 (this work, data not shown) do not affect tyrosine phosphorylation. This result was not unexpected, since it is likely that capacitation-associated events are not necessarily correlated or connected.

Since CFTR can also conduct HCO_3^- [29, 53, 54], it is not surprising that the CFTR inhibitor reduced the fast HCO_3^--induced hyperpolarization. On the other hand, the action of Tdap and 5099 on the HCO_3^--induced hyperpolarization suggests that SLC26A3 is somehow involved in this change, possibly causing a short-circuit, although unspecific effects on NBC cannot be ruled out.

Data from the literature are conflicting with respect to the hypothesis that CFTR expression, independently of its transport activity, may be sufficient to activate the expression and/or function of SLC26 transporters [55]. A recent report indicates that CFTR transport activity, and not just its presence,

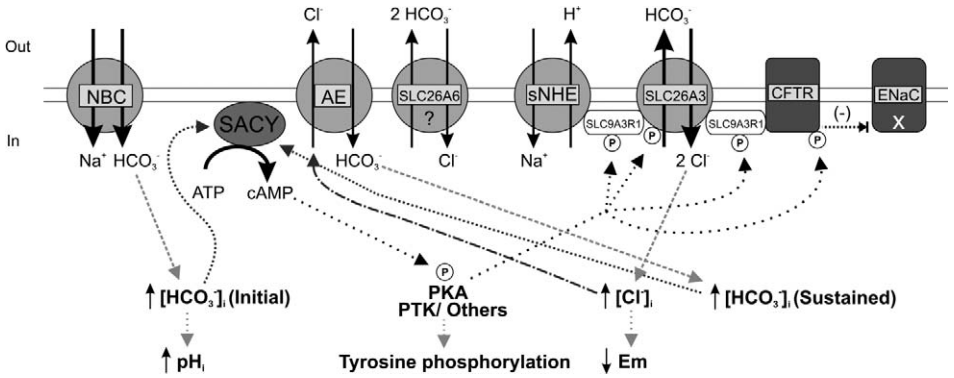

FIG. 8. Model for Cl^- and HCO_3^- movement during capacitation. Once inside the female reproductive tract, spermatozoa encounter several environmental changes. There is an external increase in HCO_3^- that could cause an initial $[HCO_3^-]_i$ elevation through NBC, provoking SACY activation and cAMP augmentation, resulting in PKA increased activity and SLC26A3/CFTR/sNHE complex stimulation via phosphorylation. This complex would transport Cl^- inside the cell, and the resulting $[Cl^-]_i$ increase would provide the driving force for the sustained uptake of HCO_3^- in exchange for internal Cl^- through an electroneutral Cl^-/HCO_3^- exchanger (AE). The sustained elevated $[HCO_3^-]_i$ would maintain high cAMP levels, which are needed for the process of capacitation that ultimately leads to a pH_i and $[Ca^{2+}]_i$ increase, tyrosine phosphorylation, and plasma membrane hyperpolarization.

is required for HCO_3^- transport via the SLC26 anion exchangers [44]. Our results using the CFTR inhibitor indicate that the CFTR functional activity regulates Cl^- transport in mouse spermatozoa.

It has been suggested that CFTR increases its permeability to HCO_3^- during sperm capacitation [7, 23]. Some groups indicate that the HCO_3^- permeability of CFTR is dynamically regulated by extracellular Cl^-. For example, in the pancreatic duct, CFTR does not transport HCO_3^- in the presence of physiological Cl^-. Only when luminal Cl^- is reduced to about 20 mmol/L (as in the stimulated duct) does CFTR switch to a higher HCO_3^- permeability contributing to HCO_3^- movement [53, 56]. On the other hand, it has been indicated that an HCO_3^-/Cl^- selectivity increase is not necessary to support HCO_3^- movement via CFTR, since the channel has a finite permeability to this anion [57]. It remains to be defined how much CFTR contributes to HCO_3^- uptake, and how it mediates Cl^- entry to spermatozoa.

Unfortunately, to date there are no direct specific inhibitors of SLC26A6. DOG and PMA, two compounds that activate PKC [35], have been used to inhibit SLC26A6, as it is phosphorylated by PKC [34]. These treatments did not affect the $[Cl^-]_i$ increase induced by db-cAMP, the capacitation-associated hyperpolarization, or the HCO_3^--induced hyperpolarization. The lack of effect of these compounds suggests that PKC and/or SLC26A6 do not have a significant involvement in these processes. It is worth mentioning that, although the cAMP/PKA signaling cascade has been shown to play an important role during capacitation [58], other kinases, such as PKC, are also present in mammalian spermatozoa and may participate in motility and during the AR [59]. Immunolocalization experiments have indicated the presence of PKC, both in the equatorial segment and in the principal piece of human sperm [60]. PKC inhibitors have been shown to reduce motility, while PKC agonists increase it [61]. Capacitation also involves the formation of an actin network between the outer acrosomal membrane and the overlying plasma membrane, and it has been proposed that PKC may participate in this process [62]. To further explore the role of PKC in these processes, we decided to investigate if PKC inhibitors (bisindolylmaleimide and chelerythrine) affect the Cl^-, Em, and pH measurements. At the concentrations used, these compounds did not affect the capacitation-associated changes in $[Cl^-]_i$, Em, or pH_i (Supplemental Fig. S2). These results suggest that PKC does not participate in these changes.

Interestingly, experiments with SLC26A3 and CFTR inhibitors suggest that these Cl^- transporters participate in the pH_i increase that accompanies capacitation. This pH_i change may be directly mediated by HCO_3^- entry or, as it was recently reported, through the interaction of SLC26 with Na^+/H^+ exchangers. For example, the interaction of SLC26A3 with NHE2 and NHE3 [44, 63–65], and the regulation of SLC26A6 by NHE3 [44, 66], has been documented. In general, it has been suggested that SLC26A3 and SLC26A6 need proton recycling via Na^+/H^+ exchangers to operate in the Cl^- absorptive mode [44]. In fact, in kidney and intestinal cells, the inhibition of SLC26A3, SLC26A6, or even CFTR causes intracellular acidification [44, 49, 66]. This mode of regulation is consistent with the observations that SLC26A3 and CFTR inhibitors blocked the capacitation-associated pH_i increase during mouse sperm capacitation.

It is worth considering the possible participation of several entry mechanisms for HCO_3^- in mouse spermatozoa: 1) a fast and transient HCO_3^- influx mediated by the NBC, favored by an abrupt increase in the extracellular bicarbonate concentration that occurs when sperm enter the female reproductive tract, where there is a high concentration of this anion; 2) a sustained increase in $[HCO_3^-]_i$, probably mediated by the SLC26/CFTR complex—this complex would facilitate Cl^- entry into the cell, creating a driving force to favor HCO_3^- uptake in exchange for Cl^-, likely through an electroneutral exchanger throughout capacitation; and 3) it has been proposed that $[HCO_3^-]_i$ increases in spermatozoa can occur via diffusion of CO_2, followed by intracellular rehydration, facilitated by carbonic anhydrases (CA) [11]. A permeable CA inhibitor (acetazolamide, which inhibits CA II) decreases flagellar beating in the presence of HCO_3^-. This effect is not seen in the presence of an impermeable inhibitor of CA (benzolamide, nonspecific inhibitor for extracellular CA) [11]. In addition, CA IV, an external CA that is present in sperm [67], may equilibrate HCO_3^- and CO_2 near the sperm surface, so that an increase in external CO_2 rapidly replenishes HCO_3^- at the extracellular membrane face, from where it can then enter the cell carried by anion transporters [68]. Therefore, HCO_3^- influx during capacitation could (at least in part) be derived from the CO_2 pathway.

Our proposed model illustrated in Figure 8 includes SLC26A3, SL26A6, and SLC9A3R1, as we have shown that they are present in mouse spermatozoa and localized to the midpiece. Although both transporters are thought to serve as

regulators of the Cl^- and HCO_3^- homeostasis during sperm epididymal maturation and capacitation, our functional experiments only support the involvement of SLC26A3 and CFTR in capacitation. It is likely that SLC26A3, CFTR, and probably sNHE are coupled, forming a transport complex. Our results with the SLC26A3 and CFTR inhibitors are consistent with this proposal. SLC26 transporters may be regulated in a similar fashion to NKCC1 [8] and KCC [69] transporters, which are functionally modulated by PKA and WNK kinases, also known to influence the SLC26 family [70–73]. The external changes in $[HCO_3^-]$ encountered by spermatozoa, upon departure from the epididymis and when entering the female tract, would cause an initial SACY activation and cAMP elevation, resulting in PKA and SLC26A3 stimulation. The increased activity of the SLC26A3/CFTR/sNHE complex would increase $[Cl^-]_i$, allowing the sustained uptake of HCO_3^- in exchange for internal Cl^- through an electroneutral Cl^- and HCO_3^- exchanger. The sustained elevated $[HCO_3^-]_i$ would maintain elevated cAMP levels needed for the process of capacitation that lead to a pH_i and $[Ca^{2+}]_i$ increase, hyperpolarization, and tyrosine phosphorylation.

Fertilization success is crucial for species preservation, and it is therefore conceivable that any given species may have several alternative mechanisms to achieve fertilization. This could explain why several knockout (KO) models of genes apparently important for fertilization produce fertile phenotypes. For instance, there are only two examples of ion channel KOs in mice that produce male infertility (CATSPER and KCNU1) [74, 75]. However, it is important to highlight that the *Slc26a3* KO mouse exhibits reduced fertility compared to wild-type mice (the number of pups is reduced by 50%); their survival rate is also low, and they have reduced size and a condition known as congenital chloride diarrhea (CLD) [45]. In humans, mutations in SLC26A3 also cause subfertility (oligoasthenoteratozoospermia) and the CLD condition [76]. In that work, the authors demonstrated that patients with mutations in SLC26A3 showed low sperm count, poor sperm motility, and a high percentage of morphological defects. A primary defect in Cl^-/HCO_3^- transport in the male reproductive tract was proposed after the observation of a high concentration of Cl^- and a low pH in the seminal plasma among these males [76].

The *Slc26a6* KO is fertile, although, interestingly, SLC26A3 is strongly upregulated in pancreas, thus causing secretin-stimulated bicarbonate secretion and pancreatic juice volume to remain unchanged in these animals [66]. It was proposed that deletion of *Slc26a6* in pancreatic duct results in a compensatory upregulation of SLC26A3, which helps maintain bicarbonate secretion and pancreatic juice volume [77]. Interestingly, the double *Slc26a3*/*Slc26a6* KO mice displayed 100% postpartum lethality before weaning. These results strongly suggest that the upregulation of SLC26A6 in the small intestine of *Slc26a3* KO mice may play an important compensatory role in electrolyte homeostasis. Other SLC26 isoforms, such as SLC26A4, SLC26A8, and SLC26A11, did not show any compensatory upregulation in the colons of *Slc26a3* KO mice [45]. SLC9A3R1-null mice die 30–35 days postpartum, and therefore fertility cannot be properly determined. The previous data support the notion that these transporters play a role during fertilization.

ACKNOWLEDGMENT

The authors thank Andres Saralegui, Jose Luis De la Vega, Yoloxóchitl Sánchez, Shirley Ainsworth, Elizabeth Mata, Marcela Ramírez, and the Confocal Unit from the Departamento de Biología Celular, Centro de Investigación y de Estudios Avanzados del Instituto Politécnico Nacional for technical assistance. They also thank Juan Manuel Hurtado, Roberto Rodríguez, Orlando Trujillo Domínguez, and Arturo Ocádiz for computer services. They are in debt to Celia Santi for helpful discussions and critical reading of the manuscript. J.C.C. was supported by the Doctorado en Ciencias Biomédicas, Universidad Nacional Autónoma de México. The authors also thank Pfizer, Inc. for Tenidap and UK-5099 donation.

REFERENCES

1. Visconti PE, Kopf GS. Regulation of protein phosphorylation during sperm capacitation. Biol Reprod 1998; 59:1–6.
2. Salicioni AM, Platt MD, Wertheimer EV, Arcelay E, Allaire A, Sosnik J, Visconti PE. Signalling pathways involved in sperm capacitation. Soc Reprod Fertil Suppl 2007; 65:245–259.
3. Xie F, Garcia MA, Carlson AE, Schuh SM, Babcock DF, Jaiswal BS, Gossen JA, Esposito G, van Duin M, Conti M. Soluble adenylyl cyclase (sAC) is indispensable for sperm function and fertilization. Dev Biol 2006; 296:353–362.
4. Visconti PE, Moore GD, Bailey JL, Leclerc P, Connors SA, Pan D, Olds-Clarke P, Kopf GS. Capacitation of mouse spermatozoa. II. Protein tyrosine phosphorylation and capacitation are regulated by a cAMP-dependent pathway. Development 1995; 121:1139–1150.
5. Demarco IA, Espinosa F, Edwards J, Sosnik J, De La Vega-Beltran JL, Hockensmith JW, Kopf GS, Darszon A, Visconti PE. Involvement of a Na^+/HCO-3 cotransporter in mouse sperm capacitation. J Biol Chem 2003; 278:7001–7009.
6. Romero MF, Boron WF. Electrogenic Na^+/HCO_3^- cotransporters: cloning and physiology. Annu Rev Physiol 1999; 61:699–723.
7. Chen WY, Xu WM, Chen ZH, Ni Y, Yuan YY, Zhou SC, Zhou WW, Tsang LL, Chung YW, Hoglund P, Chan HC, Shi QX. Cl^- is required for HCO_3^- entry necessary for sperm capacitation in guinea pig: involvement of a Cl^-/HCO_3^- exchanger (SLC26A3) and CFTR. Biol Reprod 2009; 80:115–123.
8. Wertheimer EV, Salicioni AM, Liu W, Trevino CL, Chavez J, Hernandez-Gonzalez EO, Darszon A, Visconti PE. Chloride is essential for capacitation and for the capacitation-associated increase in tyrosine phosphorylation. J Biol Chem 2008; 283:35539–35550.
9. Xu WM, Shi QX, Chen WY, Zhou CX, Ni Y, Rowlands DK, Yi Liu G, Zhu H, Ma ZG, Wang XF, Chen ZH, Zhou SC, et al. Cystic fibrosis transmembrane conductance regulator is vital to sperm fertilizing capacity and male fertility. Proc Natl Acad Sci U S A 2007; 104:9816–9821.
10. Hernandez-Gonzalez EO, Trevino CL, Castellano LE, de la Vega-Beltran JL, Ocampo AY, Wertheimer E, Visconti PE, Darszon A. Involvement of cystic fibrosis transmembrane conductance regulator in mouse sperm capacitation. J Biol Chem 2007; 282:24397–24406.
11. Carlson AE, Hille B, Babcock DF. External Ca^{2+} acts upstream of adenylyl cyclase SACY in the bicarbonate signaled activation of sperm motility. Dev Biol 2007; 312:183–192.
12. Hille B. Ion Channels of Excitable Membranes. Sunderland, MA: Sinauer Associates, Inc.; 2001.
13. Hayashi H, Suruga K, Yamashita Y. Regulation of intestinal Cl^-/HCO_3^- exchanger SLC26A3 by intracellular pH. Am J Physiol Cell Physiol 2009; 296:C1279–C1290.
14. Singh AK, Sjoblom M, Zheng W, Krabbenhoft A, Riederer B, Rausch B, Manns MP, Soleimani M, Seidler U. CFTR and its key role in in vivo resting and luminal acid-induced duodenal HCO_3^- secretion. Acta Physiol (Oxf) 2008; 193:357–365.
15. Wang Y, Soyombo AA, Shcheynikov N, Zeng W, Dorwart M, Marino CR, Thomas PJ, Muallem S. Slc26a6 regulates CFTR activity in vivo to determine pancreatic duct HCO_3^- secretion: relevance to cystic fibrosis. Embo J 2006; 25:5049–5057.
16. Hihnala S, Kujala M, Toppari J, Kere J, Holmberg C, Hoglund P. Expression of SLC26A3, CFTR and NHE3 in the human male reproductive tract: role in male subfertility caused by congenital chloride diarrhoea. Mol Hum Reprod 2006; 12:107–111.
17. Ko SB, Zeng W, Dorwart MR, Luo X, Kim KH, Millen L, Goto H, Naruse S, Soyombo A, Thomas PJ, Muallem S. Gating of CFTR by the STAS domain of SLC26 transporters. Nat Cell Biol 2004; 6:343–350.
18. Gray MA. Bicarbonate secretion: it takes two to tango. Nat Cell Biol 2004; 6:292–294.
19. Pietrement C, Da Silva N, Silberstein C, James M, Marsolais M, Van Hoek A, Brown D, Pastor-Soler N, Ameen N, Laprade R, Ramesh V, Breton S. Role of NHERF1, cystic fibrosis transmembrane conductance regulator, and cAMP in the regulation of aquaporin 9. J Biol Chem 2008; 283:2986–2996.

20. Voltz JW, Brush M, Sikes S, Steplock D, Weinman EJ, Shenolikar S. Phosphorylation of PDZ1 domain attenuates NHERF-1 binding to cellular targets. J Biol Chem 2007; 282:33879–33887.
21. Shcheynikov N, Kim KH, Kim KM, Dorwart MR, Ko SB, Goto H, Naruse S, Thomas PJ, Muallem S. Dynamic control of cystic fibrosis transmembrane conductance regulator Cl^-/HCO_3^- selectivity by external Cl^-. J Biol Chem 2004; 279:21857–21865.
22. Lamprecht G, Seidler U. The emerging role of PDZ adapter proteins for regulation of intestinal ion transport. Am J Physiol Gastrointest Liver Physiol 2006; 291:G766–G777.
23. Chan HC, Ruan YC, He Q, Chen MH, Chen H, Xu WM, Chen WY, Xie C, Zhang XH, Zhou Z. The cystic fibrosis transmembrane conductance regulator in reproductive health and disease. J Physiol 2009; 587:2187–2195.
24. Serrano CJ, Trevino CL, Felix R, Darszon A. Voltage-dependent Ca(2+) channel subunit expression and immunolocalization in mouse spermatogenic cells and sperm. FEBS Lett 1999; 462:171–176.
25. Bellve AR. Purification, culture, and fractionation of spermatogenic cells. Methods Enzymol 1993; 225:84–113.
26. Kalab P, Visconti P, Leclerc P, Kopf GS. p95, the major phosphotyrosine-containing protein in mouse spermatozoa, is a hexokinase with unique properties. J Biol Chem 1994; 269:3810–3817.
27. Garcia MA, Meizel S. Determination of the steady-state intracellular chloride concentration in capacitated human spermatozoa. J Androl 1999; 20:88–93.
28. Fraire-Zamora JJ, Gonzalez-Martinez MT. Effect of intracellular pH on depolarization-evoked calcium influx in human sperm. Am J Physiol Cell Physiol 2004; 287:C1688–C1696.
29. Stewart AK, Yamamoto A, Nakakuki M, Kondo T, Alper SL, Ishiguro H. Functional coupling of apical Cl^-/HCO_3^- exchange with CFTR in stimulated HCO_3^- secretion by guinea pig interlobular pancreatic duct. Am J Physiol Gastrointest Liver Physiol 2009; 296:G1307–G1317.
30. Broere N, Hillesheim J, Tuo B, Jorna H, Houtsmuller AB, Shenolikar S, Weinman EJ, Donowitz M, Seidler U, de Jonge HR, Hogema BM. Cystic fibrosis transmembrane conductance regulator activation is reduced in the small intestine of Na^+/H^+ exchanger 3 regulatory factor 1 (NHERF-1)- but not NHERF-2-deficient mice. J Biol Chem 2007; 282:37575–37584.
31. Kujala M, Hihnala S, Tienari J, Kaunisto K, Hastbacka J, Holmberg C, Kere J, Hoglund P. Expression of ion transport-associated proteins in human efferent and epididymal ducts. Reproduction 2007; 133:775–784.
32. Guggino WB, Stanton BA. New insights into cystic fibrosis: molecular switches that regulate CFTR. Nat Rev Mol Cell Biol 2006; 7:426–436.
33. Chernova MN, Jiang L, Shmukler BE, Schweinfest CW, Blanco P, Freedman SD, Stewart AK, Alper SL. Acute regulation of the SLC26A3 congenital chloride diarrhoea anion exchanger (DRA) expressed in *Xenopus* oocytes. J Physiol 2003; 549:3–19.
34. Hassan HA, Mentone S, Karniski LP, Rajendran VM, Aronson PS. Regulation of anion exchanger Slc26a6 by protein kinase C. Am J Physiol Cell Physiol 2007; 292:C1485–C1492.
35. Slater SJ, Kelly MB, Taddeo FJ, Rubin E, Stubbs CD. Evidence for discrete diacylglycerol and phorbol ester activator sites on protein kinase C: differences in effects of 1-alkanol inhibition, activation by phosphatidylethanolamine and calcium chelation. J Biol Chem 1994; 269:17160–17165.
36. Zeng Y, Clark EN, Florman HM. Sperm membrane potential: hyperpolarization during capacitation regulates zona pellucida-dependent acrosomal secretion. Dev Biol 1995; 171:554–563.
37. Neri-Vidaurri Pdel C, Torres-Flores V, Gonzalez-Martinez MT. A remarkable increase in the pHi sensitivity of voltage-dependent calcium channels occurs in human sperm incubated in capacitating conditions. Biochem Biophys Res Commun 2006; 343:105–109.
38. Zeng Y, Oberdorf JA, Florman HM. pH regulation in mouse sperm: identification of Na(+)-, Cl(−)-, and HCO3(−)-dependent and arylaminobenzoate-dependent regulatory mechanisms and characterization of their roles in sperm capacitation. Dev Biol 1996; 173:510–520.
39. Zhou CX, Wang XF, Chan HC. Bicarbonate secretion by the female reproductive tract and its impact on sperm fertilizing capacity. Sheng Li Xue Bao 2005; 57:115–124.
40. Gadella BM, Van Gestel RA. Bicarbonate and its role in mammalian sperm function. Anim Reprod Sci 2004; 82–83:307–319.
41. Mannowetz N, Wandernoth P, Hornung J, Ruffing U, Raubuch M, Wennemuth G. Early activation of sperm by HCO(3) (−) is regulated hormonally in the murine uterus. Int J Androl 2011; 34:153–164.
42. Chan HC, Shi QX, Zhou CX, Wang XF, Xu WM, Chen WY, Chen AJ, Ni Y, Yuan YY. Critical role of CFTR in uterine bicarbonate secretion and the fertilizing capacity of sperm. Mol Cell Endocrinol 2006; 250:106–113.
43. Ohana E, Shcheynikov N, Yang D, So I, Muallem S. Determinants of coupled transport and uncoupled current by the electrogenic SLC26 transporters. J Gen Physiol 2011; 137:239–251.
44. Singh AK, Riederer B, Chen M, Xiao F, Krabbenhoft A, Engelhardt R, Nylander O, Soleimani M, Seidler U. The switch of intestinal Slc26 exchangers from anion absorptive to HCOFormula secretory mode is dependent on CFTR anion channel function. Am J Physiol Cell Physiol 2010; 298:C1057–C1065.
45. Schweinfest CW, Spyropoulos DD, Henderson KW, Kim JH, Chapman JM, Barone S, Worrell RT, Wang Z, Soleimani M. slc26a3 (dra)-deficient mice display chloride-losing diarrhea, enhanced colonic proliferation, and distinct up-regulation of ion transporters in the colon. J Biol Chem 2006; 281:37962–37971.
46. Byeon MK, Frankel A, Papas TS, Henderson KW, Schweinfest CW. Human DRA functions as a sulfate transporter in Sf9 insect cells. Protein Expr Purif 1998; 12:67–74.
47. Byeon MK, Westerman MA, Maroulakou IG, Henderson KW, Suster S, Zhang XK, Papas TS, Vesely J, Willingham MC, Green JE, Schweinfest CW. The down-regulated in adenoma (DRA) gene encodes an intestine-specific membrane glycoprotein. Oncogene 1996; 12:387–396.
48. Alvarez BV, Vilas GL, Casey JR. Metabolon disruption: a mechanism that regulates bicarbonate transport. Embo J 2005; 24:2499–2511.
49. Lohi H, Lamprecht G, Markovich D, Heil A, Kujala M, Seidler U, Kere J. Isoforms of SLC26A6 mediate anion transport and have functional PDZ interaction domains. Am J Physiol Cell Physiol 2003; 284:C769–C779.
50. Ohana E, Yang D, Shcheynikov N, Muallem S. Diverse transport modes by the solute carrier 26 family of anion transporters. J Physiol 2009; 587:2179–2185.
51. Shcheynikov N, Wang Y, Park M, Ko SB, Dorwart M, Naruse S, Thomas PJ, Muallem S. Coupling modes and stoichiometry of Cl^-/HCO_3^- exchange by slc26a3 and slc26a6. J Gen Physiol 2006; 127:511–524.
52. Shcheynikov N, Ko SB, Zeng W, Choi JY, Dorwart MR, Thomas PJ, Muallem S. Regulatory interaction between CFTR and the SLC26 transporters. Novartis Found Symp 2006; 273:177–186; discussion 186–192, 261–174.
53. Park HW, Nam JH, Kim JY, Namkung W, Yoon JS, Lee JS, Kim KS, Venglovecz V, Gray MA, Kim KH, Lee MG. Dynamic regulation of CFTR bicarbonate permeability by $[Cl^-]i$ and its role in pancreatic bicarbonate secretion. Gastroenterology 2010; 139:620–631.
54. Yang D, Shcheynikov N, Zeng W, Ohana E, So I, Ando H, Mizutani A, Mikoshiba K, Muallem S. IRBIT coordinates epithelial fluid and HCO_3^- secretion by stimulating the transporters pNBC1 and CFTR in the murine pancreatic duct. J Clin Invest 2009; 119:193–202.
55. Ignath I, Hegyi P, Venglovecz V, Szekely CA, Carr G, Hasegawa M, Inoue M, Takacs T, Argent BE, Gray MA, Rakonczay Z Jr. CFTR expression but not Cl^- transport is involved in the stimulatory effect of bile acids on apical Cl^-/HCO_3^- exchange activity in human pancreatic duct cells. Pancreas 2009; 38:921–929.
56. Lee MG, Muallem S. Physiology of duct cell secretion. In: Beger HG, Warshaw AL, Büchler MW, Kozarek RA, Lerch MM, Neoptolemos JP, Shiratori K, Whitcomb DC, Rau BM (eds.), The Pancreas: An Integrated Textbook of Basic Science, Medicine, and Surgery, 2nd ed. Oxford: Blackwell Publishing Ltd.; 2009.
57. Ishiguro H, Steward M, Naruse S. Cystic fibrosis transmembrane conductance regulator and SLC26 transporters in HCO3(−) secretion by pancreatic duct cells. Sheng Li Xue Bao 2007; 59:465–476.
58. Visconti PE, Krapf D, de la Vega-Beltran JL, Acevedo JJ, Darszon A. Ion channels, phosphorylation and mammalian sperm capacitation. Asian J Androl 2011; 13:395–405.
59. Kalive M, Faust JJ, Koeneman BA, Capco DG. Involvement of the PKC family in regulation of early development. Mol Reprod Dev 2010; 77:95–104.
60. Rotem R, Paz GF, Homonnai ZT, Kalina M, Naor Z. Protein kinase C is present in human sperm: possible role in flagellar motility. Proc Natl Acad Sci U S A 1990; 87:7305–7308.
61. Rotem R, Paz GF, Homonnai ZT, Kalina M, Naor Z. Further studies on the involvement of protein kinase C in human sperm flagellar motility. Endocrinology 1990; 127:2571–2577.
62. Cohen G, Rubinstein S, Gur Y, Breitbart H. Crosstalk between protein kinase A and C regulates phospholipase D and F-actin formation during sperm capacitation. Dev Biol 2004; 267:230–241.
63. Talbot C, Lytle C. Segregation of Na/H exchanger-3 and Cl/HCO3 exchanger SLC26A3 (DRA) in rodent cecum and colon. Am J Physiol Gastrointest Liver Physiol 2010; 299:G358–G367.
64. Lissner S, Nold L, Hsieh CJ, Turner JR, Gregor M, Graeve L, Lamprecht G. Activity and PI3-kinase dependent trafficking of the intestinal anion

exchanger downregulated in adenoma depend on its PDZ interaction and on lipid rafts. Am J Physiol Gastrointest Liver Physiol 2010; 299:G907–G920.
65. Musch MW, Arvans DL, Wu GD, Chang EB. Functional coupling of the downregulated in adenoma Cl^-/base exchanger DRA and the apical Na^+/H^+ exchangers NHE2 and NHE3. Am J Physiol Gastrointest Liver Physiol 2009; 296:G202–G210.
66. Petrovic S, Barone S, Wang Z, McDonough AA, Amlal H, Soleimani M. Slc26a6 (PAT1) deletion downregulates the apical Na^+/H^+ exchanger in the straight segment of the proximal tubule. Am J Nephrol 2008; 28:330–338.
67. Sleight SB, Miranda PV, Plaskett NW, Maier B, Lysiak J, Scrable H, Herr JC, Visconti PE. Isolation and proteomic analysis of mouse sperm detergent-resistant membrane fractions: evidence for dissociation of lipid rafts during capacitation. Biol Reprod 2005; 73:721–729.
68. Wandernoth PM, Raubuch M, Mannowetz N, Becker HM, Deitmer JW, Sly WS, Wennemuth G. Role of carbonic anhydrase IV in the bicarbonate-mediated activation of murine and human sperm. PLoS One 2010; 5:e15061.
69. Klein T, Cooper TG, Yeung CH. The role of potassium chloride cotransporters in murine and human sperm volume regulation. Biol Reprod 2006; 75:853–858.
70. Muallem D, Vergani P. Review. ATP hydrolysis-driven gating in cystic fibrosis transmembrane conductance regulator. Philos Trans R Soc Lond B Biol Sci 2009; 364:247–255.
71. Kahle KT, Ring AM, Lifton RP. Molecular physiology of the WNK kinases. Annu Rev Physiol 2008; 70:329–355.
72. Yang CL, Liu X, Paliege A, Zhu X, Bachmann S, Dawson DC, Ellison DH. WNK1 and WNK4 modulate CFTR activity. Biochem Biophys Res Commun 2007; 353:535–540.
73. Gamba G. WNK lies upstream of kinases involved in regulation of ion transporters. Biochem J 2005; 391:e1–e3.
74. Santi CM, Martinez-Lopez P, de la Vega-Beltran JL, Butler A, Alisio A, Darszon A, Salkoff L. The SLO3 sperm-specific potassium channel plays a vital role in male fertility. FEBS Lett 2010; 584:1041–1046.
75. Ho K, Wolff CA, Suarez SS. CatSper-null mutant spermatozoa are unable to ascend beyond the oviductal reservoir. Reprod Fertil Dev 2009; 21:345–350.
76. Hoglund P, Hihnala S, Kujala M, Tiitinen A, Dunkel L, Holmberg C. Disruption of the SLC26A3-mediated anion transport is associated with male subfertility. Fertil Steril 2006; 85:232–235.
77. Ishiguro H, Namkung W, Yamamoto A, Wang Z, Worrell RT, Xu J, Lee MG, Soleimani M. Effect of Slc26a6 deletion on apical Cl^-/HCO_3^- exchanger activity and cAMP-stimulated bicarbonate secretion in pancreatic duct. Am J Physiol Gastrointest Liver Physiol 2007; 292:G447–G455.